Received: 14 March 2022 | Revised: 6 May 2022 | Accepted: 20 May 2022

DOI: 10.1002/term.3326

WILEY

RESEARCH ARTICLE

Application of suture anchors for a clinically relevant rat model of rotator cuff tear

Yang Liu[1,2,3,4] | Sai-Chuen Fu[2,5] | Shi-Yi Yao[2] | Xiao-Dan Chen[2] | Patrick Shu-Hang Yung[2]

[1]Department of Bone and Joint Surgery, Shenzhen People's Hospital, Shenzhen, Guangdong, China

[2]Department of Orthopaedics and Traumatology, Faculty of Medicine, The Chinese University of Hong Kong, Hong Kong SAR, China

[3]The Second Clinical Medical College, Jinan University, Shenzhen, Guangdong, China

[4]The First Affiliated Hospital, Southern University of Science and Technology, Shenzhen, Guangdong, China

[5]Lui Che Woo Institute of Innovative Medicine, The Chinese University of Hong Kong, Hong Kong SAR, China

Correspondence
Patrick Shu-Hang Yung, Room 74029, 5/F, Lui Che Woo Clinical Science Building, Prince of Wales Hospital, Shatin, NT, Hong Kong, China.
Email: patrickyung@cuhk.edu.hk

Abstract

Current rat model of rotator cuff (RC) tear could not mimic the suture anchor (SA) repair technique in the clinical practice. We designed a novel SA for RC repair of rats to establish a clinically relevant animal model. Small suture anchors that fit the rat shoulder were assembled. 60 rats were assigned to the transosseous (TO) repair group or SA repair group ($n = 30$/group). Micro-computed tomography (Micro-CT) scanning, biomechanical test and histological analysis were implemented at 2, 4, and 8-week post-repair. The failure load and stiffness in the SA group were significantly higher than those of TO group at 4-week post-repair. Micro-computed tomography analysis showed the bone mineral density and trabecular thickness of the SA group were significantly lower than those of TO group. The SA group showed a better insertion continuity at 4-week post-repair compared to TO group. No significant difference in gait parameters was found between groups. Therefore, SA repair is applicable for the rat model of RC tears. The SA repair achieved superior RC tendon healing, but more extensive initial bone damage compared to TO repair, while the shoulder function was comparable. This model could replicate the current repair technique in the clinical situation and be considered for future preclinical studies on healing enhancement for RC tears. **Statement of Clinical Significance**: With high clinical relevance, this model may facilitate the translation from an animal study into clinical trials.

KEYWORDS
animal, models, rotator cuff injuries, suture anchors

1 | INTRODUCTION

The incidence of the rotator cuff (RC) tear is high and increasing with age. It has been reported that 49.5% of the population above 60-year-old suffered RC tear (Yamamoto et al., 2010). The main symptoms of RC tears are pain and dysfunction of the shoulder, which will reduce the patient's ability to perform daily activities, such as axilla wash, hair comb, perineal care, and upward reach (Vidt et al., 2016). Up to 93% of the patients with symptoms cannot lift heavy things. Therefore, the RC tear negatively impact the patients' quality of life.

Once the RC tendon is completely torn, it will not heal without surgical repair (CJ & K, 2002), after which the shoulder function will recover up to 70% (McElvany et al., 2015). However, clinical data showed that 21–26.6% of the patients with small or medium tears

(<3 cm) suffered retear of the RC tendon. The rate increased to 94% in patients with massive tears (>5 cm) (Bedeir et al., 2018; Moosmayer et al., 2019; Vastamaki et al., 2013). The poor healing of the RC tendon associates with poor shoulder function, especially for massive retear patients in the long term. Hence, the poor healing outcome of RC repair remains a significant concern. Strategies for improving healing are urgently demanded.

Rat RC tear model has been widely used in previous preclinical studies on enhancements of tendon-to-bone healing (Bedi et al., 2010; Kovacevic et al., 2011; Min et al., 2016; Yonemitsu et al., 2019). However, biological enhancements proved effective in animal studies has seldomly translated into clinical practice. It might be due to the differences between the animal model and the human condition (Mergenthaler & Meisel, 2015). Although the rat model is well developed for RC repairs, the tendon repair technique on this model varies from that of the up-to-date clinical practice. Currently, the primary technique of tendon fixation for clinical RC repair is suture anchor (SA) (Visscher et al., 2019). While in the rat models, the transosseous (TO) bone tunnel technique has been commonly applied (Denard & Burkhart, 2013; Visscher et al., 2019). Different techniques could lead to a different mechanical and biological environment of the repair site, thereby influencing the shoulder's healing outcome and functional recovery (Burkhart et al., 1997; Ficklscherer et al., 2014; Levy et al., 2013; Park et al., 2005).

Therefore, a modified rat RC model incorporated the surgical technique of clinical relevance is needed. Since the rat shoulders are so small that the commercially available SA cannot fit in, we proposed a custom-made SA suitable for rats. Hence, this study aimed to develop a rat model of RC tears repaired with SA and compare the healing outcome and functional recovery of the shoulder with the conventional TO technique. We hypothesized that the SA repair is applicable, and it might show better healing outcomes and shoulder functions than the TO repair.

2 | MATERIALS AND METHODS

The research protocol has been approved by the Animal Experimentation Ethics Committee in the Chinese University of Hong Kong (Ref. No. 19-141-MIS).

2.1 | Preparation of the SA

Based on the design of the commercially available all-suture anchor (Barber & Herbert, 2017), the SA for rats was assembled with a section of suture which was 12 cm in length (5-0 Vicryl™, Ethicon, Inc, New Jersey, USA) crookedly passing through a section of suture (#0 Vicryl™, Ethicon, Inc, New Jersey, USA) which was 8 mm in length. The thin thread was passed through the thick thread with three interwoven sutures (Figure 1). A hole (⌀ 0.9 mm) was drilled on the insertion area at the greater tuberosity of the humeral head. Then, the SA was inserted until the anchor fully engaged with the cortical bone (Figure 2).

2.2 | The RC tear model

Sixty male adult Sprague-Dawley rats (400–450g) were randomly assigned to the TO and SA repair groups (n = 30). The rats for the current study were obtained from the animal center in the Chinese University of Hong Kong and held in the animal house at the Prince of Wales Hospital. Four rats were held together in a standard plastic rat cage. The study design is shown in Figure 3.

Anesthesia was performed with an intraperitoneal injection of ketamine (75 mg/kg) and xylazine (10 mg/kg). Subcutaneous injection of buprenorphine (0.05 mg/kg) was administrated for pain relief 15 min before the operation. Rats received operations in the supraspinatus (SS) tendon on the right shoulder by the same operator.

A 1.5 cm skin incision was made longitudinally above the acromial in a supine position. The deltoid muscle was split along the direction of muscle fibers to expose the SS tendon, identified as a bright tendon that reached out below the acromion and inserted onto the greater tuberosity. The SS tendon was isolated and transected from its bony insertion with a No.15 scalpel. A suture marker was made at the distal end of the SS stump using a section of 8 mm 5-0 Prolene™ (Ethicon, Blue Ash, Ohio, USA). The incision was then closed in layers.

After surgery, the rats were kept separately for 24 h and fed *ad libitum*, allowing free cage activities after recovering from anesthesia. Buprenorphine (0.05 mg/kg) was injected subcutaneously every 12 h for 72 h.

2.3 | Surgical procedure of RC repairs

Sixty rats and six pairs of fresh cadaver shoulder samples from rats received the SA and TO repair.

2.3.1 | The TO repair

Four weeks after the RC tear, the TO repair surgery was implemented. Scar tissues between the tendon stump and greater tuberosity were identified and excised. The SS tendon was mobilized from surrounding tissues until it approximated the anatomical insertion site on the greater tuberosity. After removing the suture marker, the distal end of the tendon (2 mm from the insertion) was stitched with 5-0 Vicryl™ suture with the Modified Mason-Allen stitches (Gerber et al., 1994). Two bone tunnels were hand-drilled by a new spherical drill bit (Ø 0.45 mm), cooling by normal saline, longitudinally at the tendon's footprint with a 2 mm distance between each other and guided out from the lateral humeral neck. The sutures were passed through the bone tunnels and fixed with five knots without tension (Figure 4). The incision was then closed in layers.

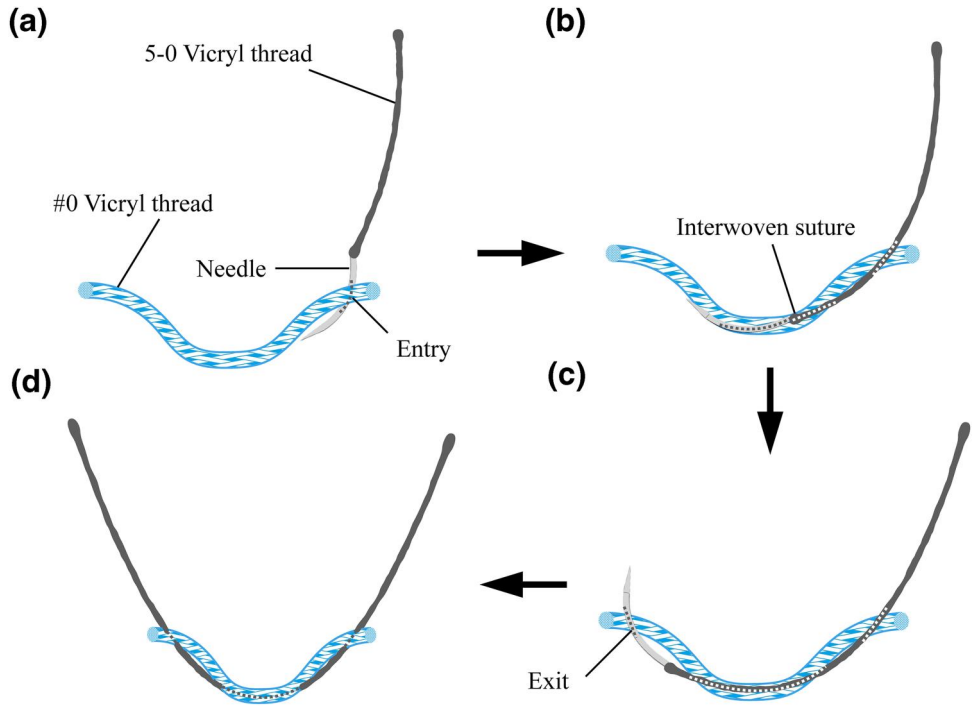

FIGURE 1 Assembling procedure of the suture anchor (SA) for the rat model. (a) The needle attached with 5-0 Vicryl thread passes through a section of #0 Vicryl thread at 1 mm to the right end. (b) The needle re-enters the #0 thread at 2 mm to the right end and forwards inside the thread along the long axis for 4 mm, then exit the thread at 2 mm to the left end. (c) The needle passes through the #0 thread at 1 mm to the left end of the thread. (d) The SA is completed

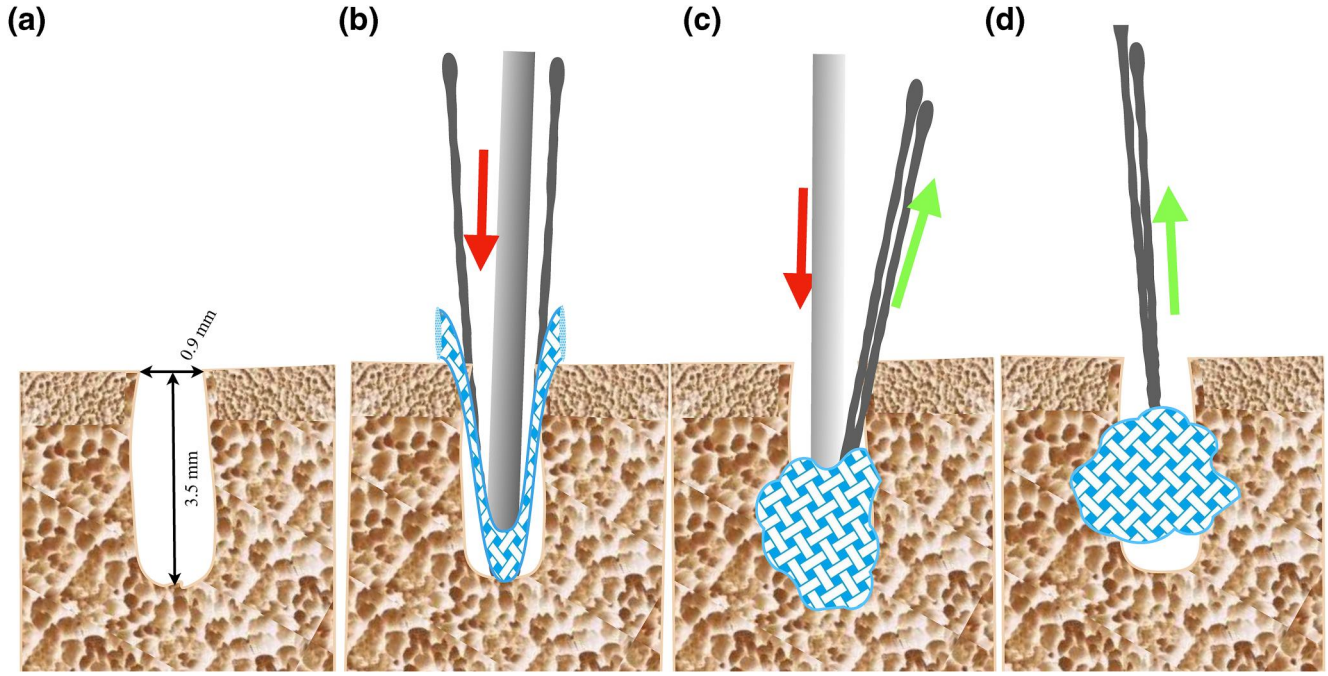

FIGURE 2 The schematic diagram showed the design of suture anchor (SA). (a) A bone site was prepared with a ∅ 0.9 mm drill bit. (b) The SA was inserted into the hole. (c) With contraction force applied to the suture, the anchor-like part was squeezed and (d) stuck in the bone site

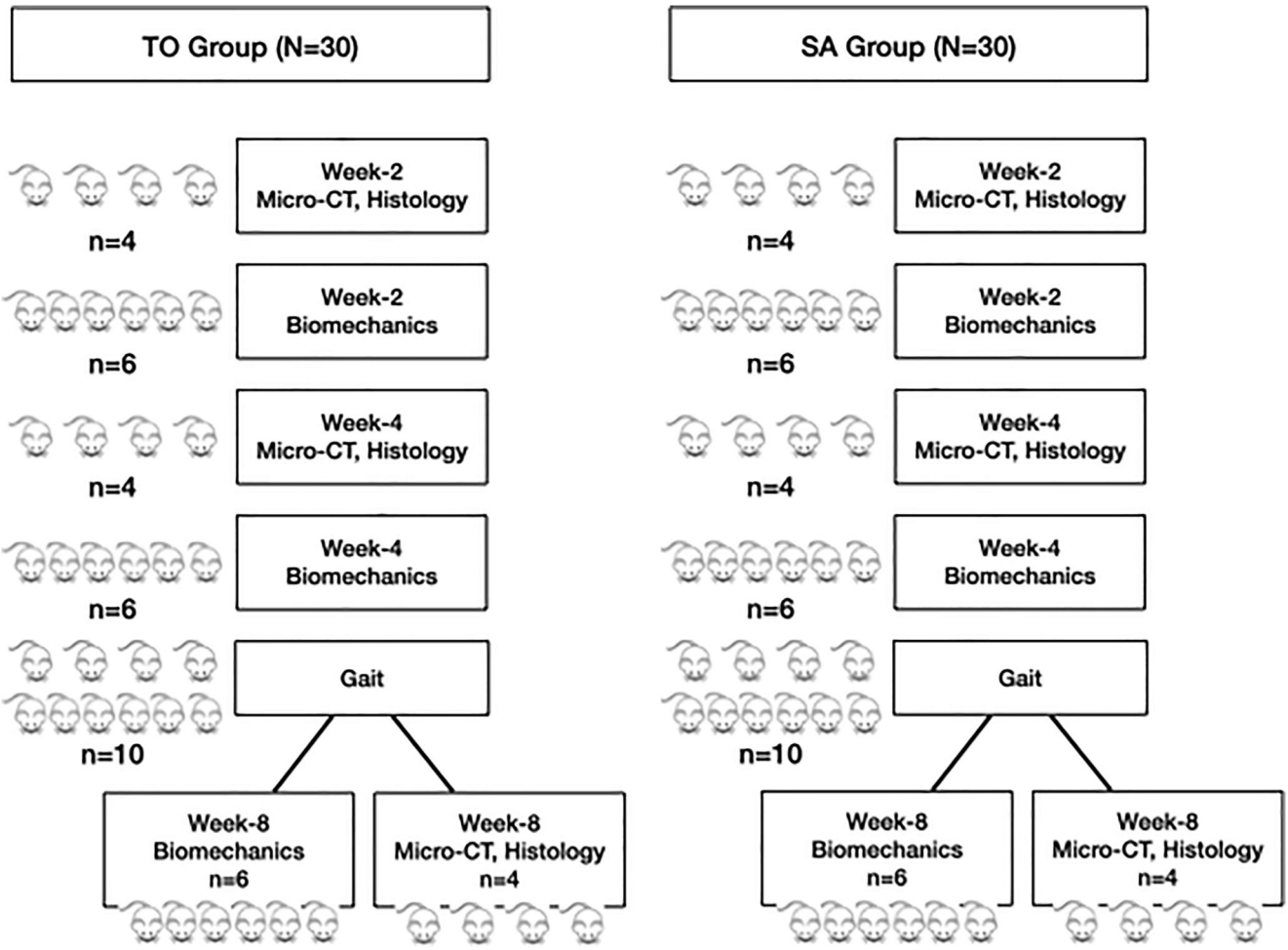

FIGURE 3 60 rats were randomly assigned into the transosseous (TO) and suture anchor (SA) group. 10 rats were euthanized at 2-, 4-, 8-week post repair. TO: transosseous; SA: suture anchor

2.3.2 | The suture anchor repair

The surgical procedure was adapted from previous studies (Barros et al., 2010; Kang et al., 2013). A hole (Ø 0.9 mm, 3 mm depth) was created with a drill bit at 45° to the long axis of humerus, in which the SA was inserted. Then, threads of the SA were stitched through the tendon stump. The sutures were fastened with five knots, and the SS tendon was pulled back onto the insertion.

2.4 | Functional assessment

At each endpoint, gait analysis was carried out in the morning. The downhill walking gait analysis was performed by CatWalk™ XT 9.0 (Noldus, Netherlands), with the right end of the walkway tilted up for 10° (Fu et al., 2012). Rats were allowed to walk voluntarily back and forth from the right end of the walkway. Each animal should at least finish two compliant walks, which was defined with speed variation less than 30%. To eliminate potential influences introduced by walking speed, the speed of each walk was recorded. Once a rat entered the region of interest (10 × 60 cm), it triggered the detection system to record the pawprint images by a digital camera set at 60 cm below the walkway. The max intensity, pawprint area, stride length and swing duration of a forelimb were automatically calculated by built-in software. All gait parameters were presented as a ratio between the operated and the control (the contralateral intact side of each rat) side in a trial to control individual variations.

2.5 | Sample collection

At each endpoint (2, 4, and 8 week post-repair), shoulder segments (upper forelimb and the whole scapular) were collected according to the requirements of the following analyses.

2.6 | Micro-CT analysis

The specimens were fixed in 10% neutral buffered formalin for 24 h and transferred to 70% ethanol at room temperature. The shoulder samples were carefully dissected and inserted vertically into the micro-CT (micro-CT 40 Scanco Medical, Brüttisellen, Switzerland).

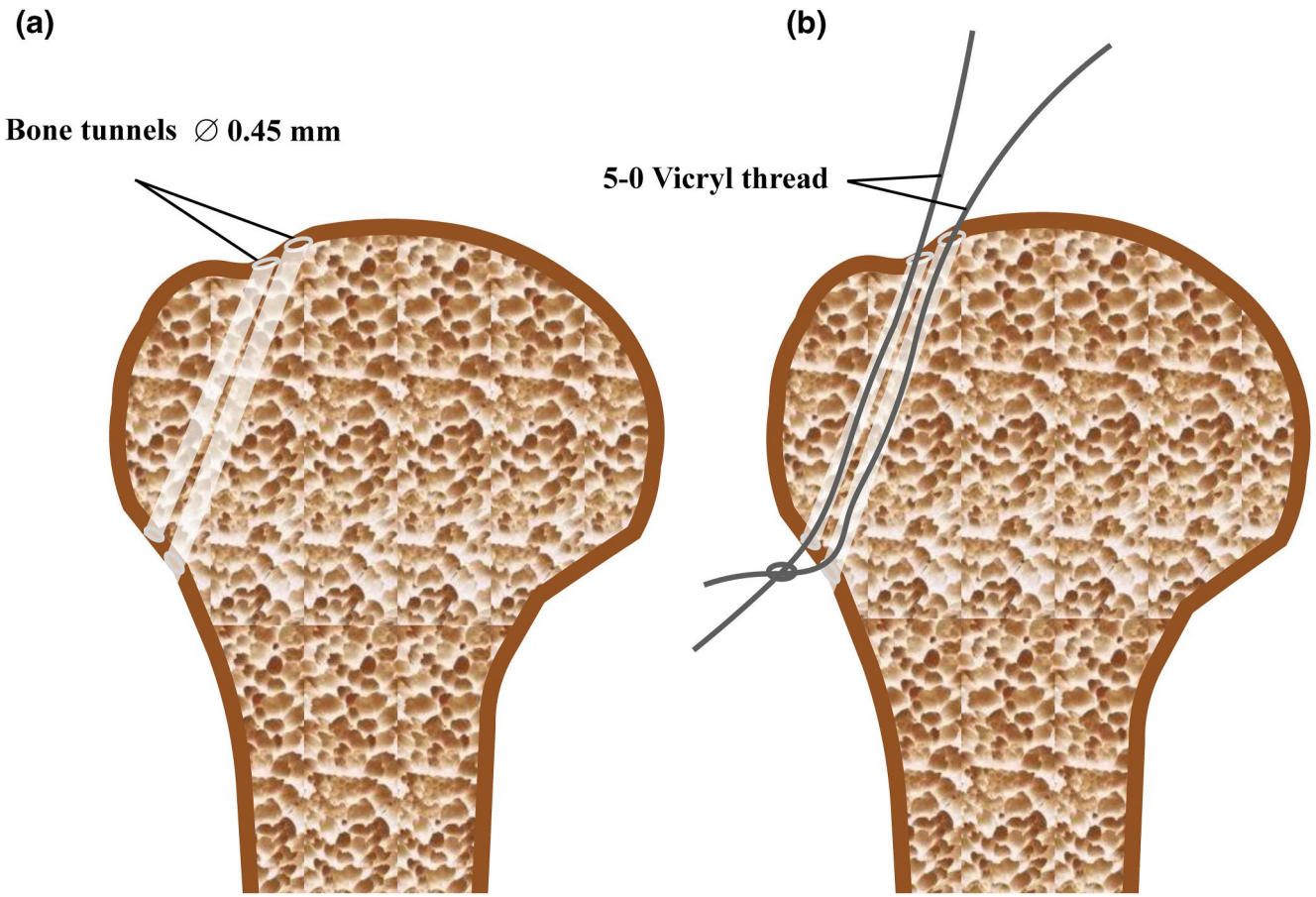

FIGURE 4 The schematic diagram showed the design of bone tunnels made in the humeral head

The volume of interest spanned from the proximate end of the greater tuberosity to 7.2 mm distal of the humerus, which included the whole humeral head. The resolutions were set with 18 μm per voxel and 1024 × 1024 pixels. Four hundred consecutive scans were performed (45 kV, 175 mA, 300 ms), and three-dimensional reconstruction was implemented with a low pass Gaussian filter (Sigma = 0.8, Support = 2). Following parameters of the trabecular region were measured: bone volume (BV) fraction (BV/total volume; BV/TV), trabecular thickness (Tb. Th), trabecular separation (Tb. Sp), trabecular number (Tb. N) and bone mineral density (BMD).

2.7 | Biomechanical tests

Ex vivo tests were performed to evaluate the pull-out strength of the anchor from the bone before connecting to the tendon. Then, cadaver shoulder samples that repaired with TO and SA technique were used to test the primary fixation strength.

For in vivo analyses, shoulder samples harvested at each time-point were send for load-to-failure test. The rat humerus was held vertically with a custom-made jig. The attached thread of the SA was directly held by a screw jig that connected to a 250 N load cell, while the jig held the repaired SS tendon with a folded blotting paper. Distance between the holding point of the SS tendon and the top of the humeral head was standardized at 2 mm. The specimen was preloaded with 0.1 N and pulled along the long axis of the humerus with 40 mm/min until failure by a universal material testing machine (Hounsfield H25K-S, Tinius Olsen Ltd, United Kingdom). The failure mode was recorded. The failure load and stiffness were recorded as raw values and transformed into the ratio of the operated and control side, respectively.

2.8 | Histology analysis

Specimens were fixed in 30° abduction of the glenohumeral joint angle with 10% neutral buffered formalin for 24 h, followed by demineralization in 10% formic acid for 14 days. As the footprint of SS tendon was not placed at the center of the surface of a humeral head, the orientation of specimens was adjusted according to desired sectioning plane. The specimen was embedded with the scapular facing down while the distal humerus tilted up for 30°. Sectioning was conducted from anterior to posterior of the humeral head with a microtome (RM 2165, Leica, Wetzlar, Germany). Tissues were trimmed off until the anterior border of the SS tendon appeared, where was set as initial position of sectioning. Three

consecutive sections with an interval of 250 μm were collected and stained with Hematoxylin and Eosin (H&E) staining. The quality of sectioning and staining was checked with a microscope (Leica DM 500, Wetzlar, Germany). The specimens were recorded with a random number and assessed blindly by two operators independently (Yang LIU and Xiaodan CHEN). Two regions of interest (ROI), including the tendon-bone interface in the greater tuberosity and the SS tendon proper, were defined (200 × 200 μm). The insertion continuity and insertion histology were evaluated according to the first ROI (interface area). The cellularity, vascularity, cell orientation, and collagen orientation were evaluated according to the second ROI (tendon proper). Six parameters were graded from 1 (closest to normal) to 4 (most abnormal) (Table 1) (Lipner et al., 2015). The maturity score was a sum of the six parameters which represented the extend of healing of the tendon-to-bone construct. The final score was the average score of the two assessors. The consistency of the scoring between the two assessors was evaluated with Kappa analysis.

2.9 | Statistical analysis

The statistical analyses were performed with SPSS Version 25 (IBM Corp, Armonk, NY, USA). Parameters were checked for normality by the Shapiro-Wilk test. The effect of surgical techniques on the shoulder function was evaluated by the repeat measured analysis of variation. The effect of surgical techniques on the mechanical, bone quality, and histological properties were analyzed with unpaired *t*-test or Mann–Whitney *U* test. The level of significance was set at $\alpha = 0.05$.

3 | RESULTS

All rats survived the surgery, and no wound complications were found. 10 rats in each group were euthanized at 2-, 4-, and 8-week post repair. At each timepoint, six out of 10 rats' shoulder samples were processed for biomechanical analysis, and the rest four shoulder samples underwent micro-CT and histological analysis. 10 rats from each group were performed with gait analysis at baseline, 4-week post tear and 2-, 4-, 8-week post repair.

3.1 | Functional assessment

The normality of distribution and equal variance were both tested. The pooled walking speed at the baseline was 27.4 ± 1.0 cm/s. No significant difference of walking speed was found at baseline between groups ($p = 0.736$). No significant decrease of the walking speed of the TO group was noticed except at 1-week after repair ($p = 0.005$), while the speed at all timepoints after SA repair were found significantly slower compared to the baseline. However, no significant difference was found between groups at all timepoints.

TABLE 1 Grading of the histological parameters

Parameters	1	2	3	4
Insertion continuity	>75%	51%–75%	26%–50%	<25%
Insertion histology	With regularity, fibrocartilage, and tidemark	With regularity and fibrocartilage but lack tidemark	With regularity but lacks fibrocartilage and tidemark	Lacks fibrocartilage, regularity, and tidemark
Cellularity	Close to normal	2 times of normal	4 times of normal	>4 times of normal
Vascularity (×25)	<6 blood vessels	6–10 blood vessels	11–15 blood vessels	>15 blood vessels
Cells parallel	>75%	51%–75%	26%–50%	<25%
Collagen orientation	>75%	51%–75%	26%–50%	<25%

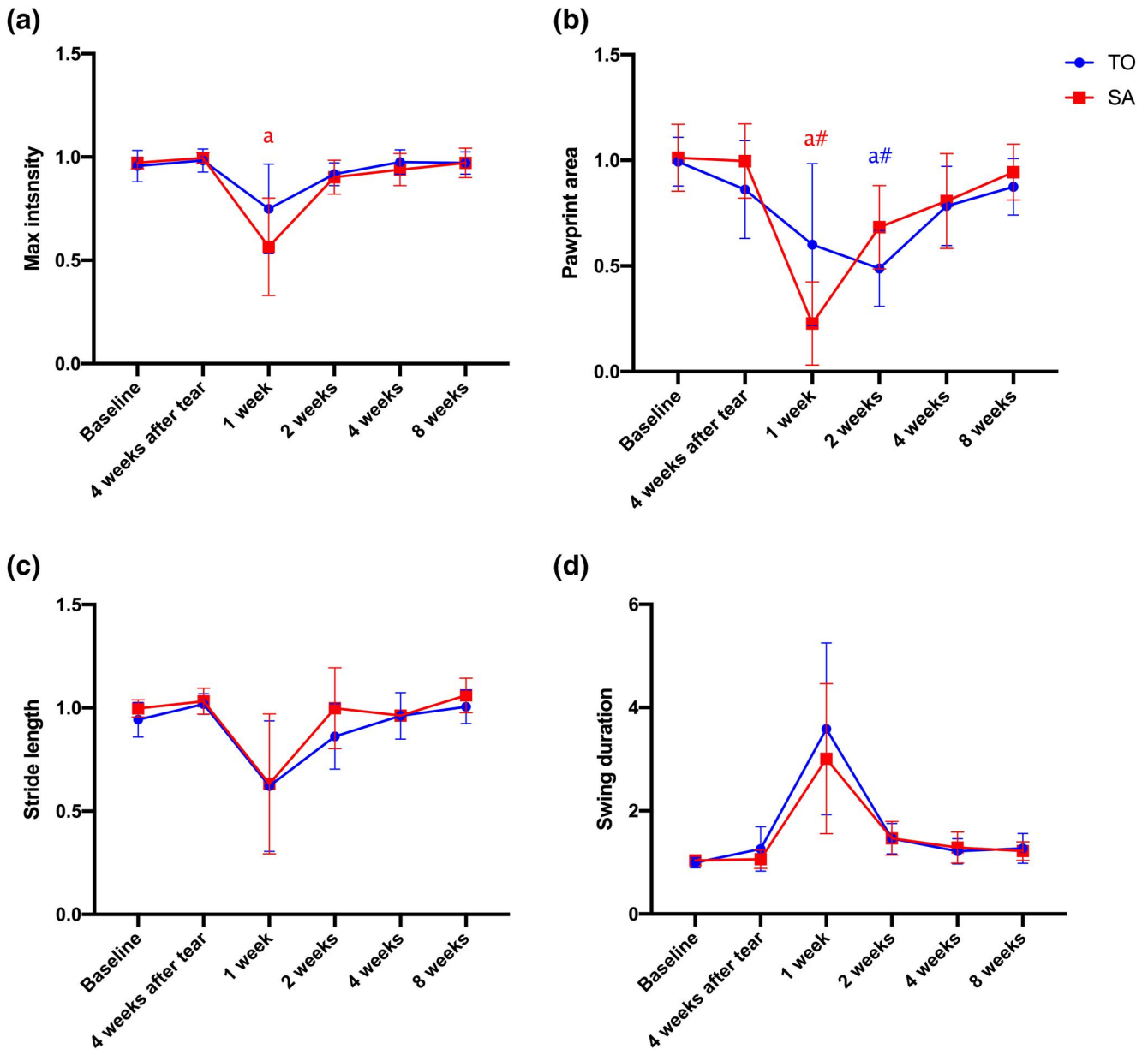

FIGURE 5 Results of the gait analysis were presented as a ratio between the operated and contralateral sides. (a) The max intensity of the suture anchor (SA) group decreased significantly at the first-week post repair than that of 4-week post tear. (b) The pawprint area dropped significantly at 1- and 2-week post repair in both groups. (c, d) The stride length and swing duration showed a similar trend. They decreased at 1-week post repair for both groups and restored at 2-week post repair. TO: transosseous; SA: suture anchor. #: $p < 0.05$ compared to 4-week post tear. a: $p < 0.05$ compared to baseline. Error bar: 95% confidence interval

No significant difference of the parameters was found between the TO and SA group in all timepoints in the downhill walking gait analyses. At 4-week post tear, all gait parameters restored to the baseline level (Figure 5). At 1-week post repair, all gait parameters were affected, especially the max intensity ($p = 0.047$) and pawprint area ($p = 0.002$) of the SA group were significantly decreased compared to those of 4-week post tear. At 2-week post repair, the pooled data of pawprint area of both groups (0.59 ± 0.26) remained significantly lower than baseline (1.00 ± 0.19, $p = 0.001$).

3.2 | Micro-CT analysis

BV/TV, Tb. Th and BMD of the SA group were significantly lower than those of the TO group (BV/TV: $p = 0.046$; Tb. Th: $p = 0.023$; BMD: $p = 0.015$). For the SA group, at 2-week post repair, the BV/TV (0.06 ± 0.02, $p = 0.009$) and BMD (150.32 ± 34.99 mgHA/cm^3, $p = 0.002$) decreased significantly compared to the baseline (BV/TV: 0.22 ± 0.03, BMD: 287.96 ± 26.16 mgHA/cm^3). They restored gradually but remained lower than baseline upon endpoint (BV/TV: 0.16 ± 0.12; BMD: 217.07 ± 69.93 mgHA/cm^3). No significant

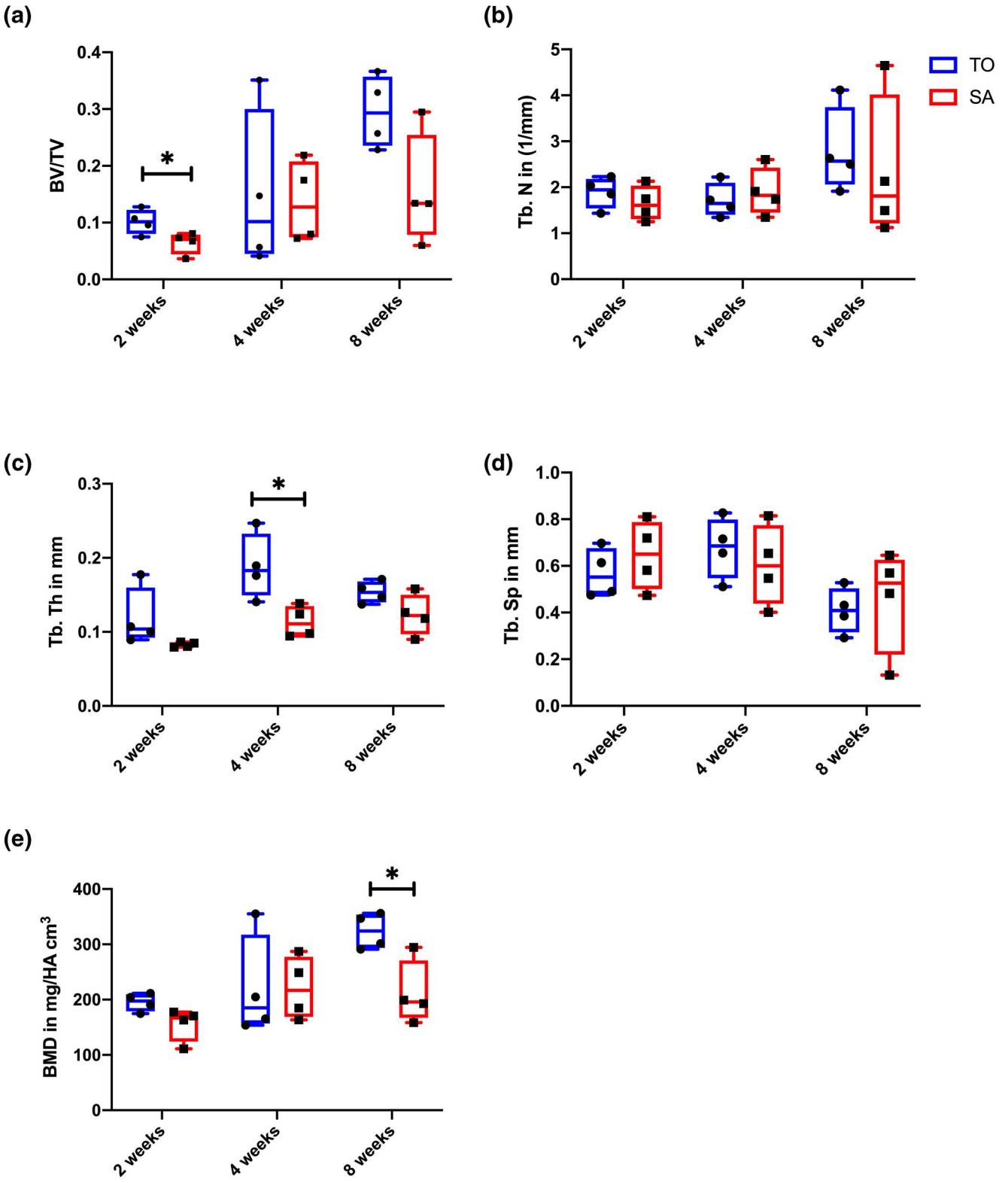

FIGURE 6 (a) An increasing trend of BV/TV was observed after repair. The suture anchor (SA) group was significantly lower than the the transosseous (TO) group at 2-week post repair. (b) No significant difference of Tb.N was found between groups. (c) Tb.Th of the SA group was significantly less than the TO group at 4-week post repair. (d) No significant difference of Tb. Sp was found between groups. (e) The bone mineral density (BMD) of the TO group was significantly higher than the SA group at 8-week post repair. TO: transosseous; SA: suture anchor. BV: bone volume; TV: tissue volume; Tb. N: trabecular number; Tb. Th: trabecular thickness; Tb. Sp: trabecular separation; BMD: bone mineral density; HA: hydroxyapatite.*: $p < 0.05$

difference was found for the TO group between each timepoint and baseline (Figure 6).

3.3 | Biomechanical analysis

3.3.1 | Ex vivo analyses

The pull-out strength of the anchor from the bone ranged from 12.7 to 16.9 N (mean: 14.77 N, standard deviation: 1.46). All ruptures took place at the suture, and no displacement of the anchor was observed. Then, cadaver shoulder samples were repaired by TO and SA technique. The primary fixation strength of the SA group (ratio of failure load: 0.14 ± 0.10; ratio of stiffness: 0.14 ± 0.08) showed no significant difference with the TO group (ratio of failure load: 0.15 ± 0.03, $p = 0.56$; ratio of stiffness: 0.17 ± 0.06, $p = 0.15$). For both groups, rupture took place at the suture-tendon interface, without any displacement of the anchor or loosening of the knots.

3.3.2 | In vivo analyses

For both groups, the ratio of failure load and stiffness have significantly increased from 2- to 8-week post repair ($p < 0.001$). The ratio of failure load increased from 0.18 ± 0.60 to 0.58 ± 0.12 in the TO group and from 0.19 ± 0.05–0.57 ± 0.24 in the SA group, while the ratio of stiffness increased from 0.13 ± 0.06–0.42 ± 0.20 in the TO group and from 0.13 ± 0.05–0.41 ± 0.17 in the SA group. The ratio of failure load and stiffness of the SA group were significantly higher than those of the TO group at 4-week post repair (ratio of failure load: $p = 0.029$, ratio of stiffness: $p = 0.02$) but comparable at 8-week post repair (Figure 7). Thirty three out of 36 control samples tore cohesively at the tendon proper, while the other three samples failed with an avulsion at the greater tuberosity. All the repaired specimens ruptured at the tendon-bone interface.

3.4 | Histological analyses

The agreement of histological scores between the two assessors was substantial, with a Kappa Coefficient of 0.732 (95% CI: 0.622–0.842).

In gross observation, no rupture or loose of the sutures or pull out of the suture anchors were observed. Swelling of the SS tendon was noticed in both groups at 2-week post repair, while it remained remarkable in the TO group at 4-week post repair. The microscopical observation was shown in Figure 8. Significant histologic differences were noticed between TO and SA specimens at 4-week post repair ($p = 0.029$), when the SA group showed a better insertion continuity, and more organized cell arrangement (Table 2). Healing of the tendon-bone unit was remarkable over time in the SA group, as demonstrated by the maturity score decreased from 19.5 (2-week post repair) to 10 (8-week post repair, $p = 0.01$). For the TO group,

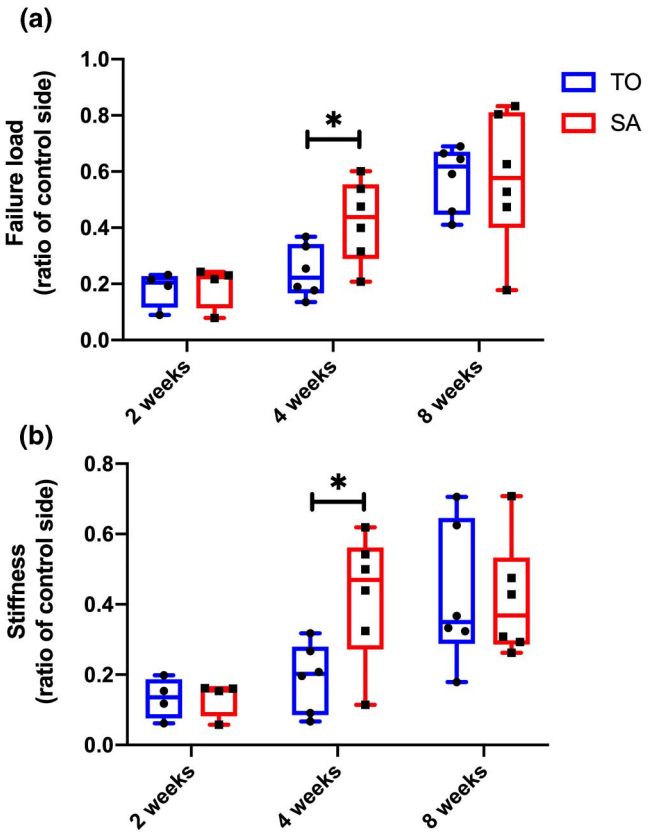

FIGURE 7 The ratio of failure load and stiffness of the suture anchor (SA) group was significantly higher than those of the the transosseous (TO) group at 4-week post repair. TO: transosseous. SA: suture anchor. *$p < 0.05$

healing of the unit was noticed, with the maturity score decreased from 16.25 (2-week post repair) to 15.5 (8-week post repair) though the change was not statistically significant.

Both groups showed significantly disorganized fibro-vascular tissue without any continuous fiber. At 8-week post repair, the orientation of the collagen fibers became more regular, with immature perforation fibers running at the tendon-bone interface. No distinctive zonal structure of fibrocartilage or Sharpey fiber was found.

4 | DISCUSSION

To the best of the authors' knowledge, SA repair on rat RC tear models has not been reported in previous studies. Only larger animals like rabbits or sheep have been employed for SA repair (Easley et al., 2020; Harrison et al., 2000; Kang et al., 2013). However, the shoulder structure of rats was considered most alike to the humans (Soslowsky et al., 1996). The current study has successfully developed the SA technique for rats, which has been commonly used in clinical practice. Therefore, rat models with this novel technique can be employed in the future studies on RC tear with better clinical relevance, lower labor, and financial cost.

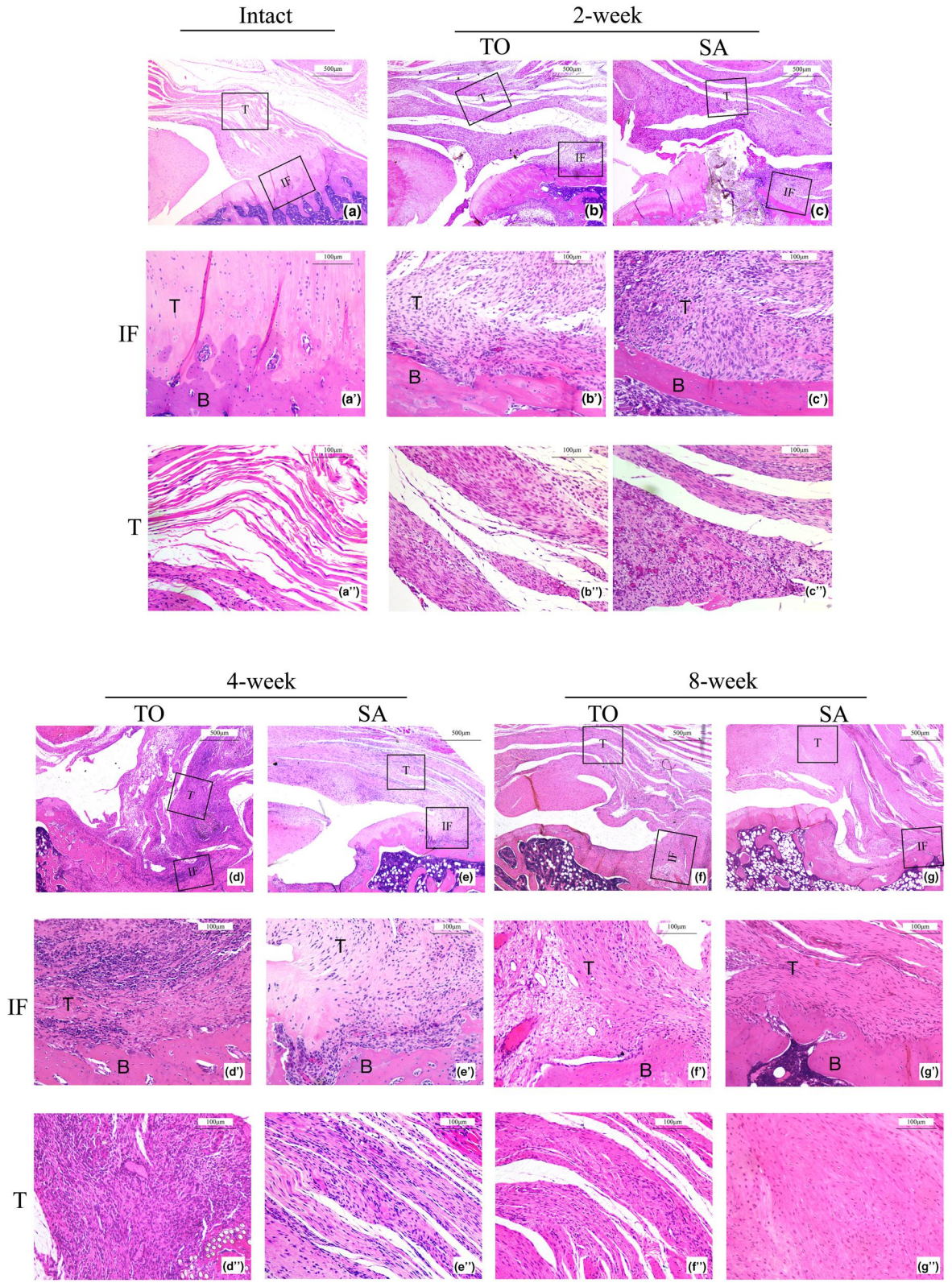

FIGURE 8 (a) Typical zonal structure of the enthesis in the intact control. A layer of mineralized fibrocartilage lies between the fibrocartilage and bone (a′). (b, c) In both groups, the continuity of the insertion was not well restored after repair (less than 50%). (f′, g′) No typical enthesis with fibrocartilage and mineralized fibrocartilage layers were formed at 8 weeks. (c″) After suture anchor (SA) repair, cell proliferation and inflammatory response were observed at 2-week post repair with increased cellularity and poorer cell orientation and collagen arrangement. These alternations improved at 4 weeks (e″) and 8 weeks (g″). The cell proliferation and inflammation were evident in the TO repair group at 2-week post repair (b″) and 4-week post repair (d″) and improved at 8-week post repair (f″). The tendon-bone healing improved significantly with time ($p = 0.001$) for the SA group, while not significant for the TO group. The insertion continuity and cells parallel for the SA group were superior to those of the TO group at 4-week post repair ($p = 0.029$). Abbreviations: B, bone; IF, interface; T, tendon proper

TABLE 2 Histological scoring of the repair site of the transosseous (TO) and suture anchor (SA) repair group (Median, range)

Parameter	Group	Intact control	2-week	4-week	8-week
Insertion continuity	TO	1 (1, 1)	3 (1.5, 3.5)	3.5 (3.5, 4)	3.25 (1.5, 4)
	SA		3 (1, 4)	1.75 (1.5, 2.5)*	1 (1, 2.5)
Insertion histology	TO	1 (1, 1)	3 (3, 3.5)	3.75 (3, 4)	3.25 (3, 4)
	SA		4 (3.5, 4)*	3.25 (3, 4)	3 (3, 3)#
Cellularity	TO	1 (1, 1)	4 (3, 4)	4 (3, 4)	2.5 (2, 3.5)
	SA		4 (3, 4)	2.25 (1.5, 3.5)	2 (2, 2.5)#
Vascularity	TO	1 (1, 1)	2 (1.5, 3.5)	1.5 (1.5, 2.5)	1.5 (1.5, 3)
	SA		2.75 (1.5, 3)	2 (2, 3)	1.5 (1.5, 2)
Cells parallel	TO	1 (1, 1)	2.75 (1.5, 4)	3.75 (3, 4)	2.75 (1.5, 3.5)
	SA		3.75 (3, 4)	1.75 (1.5, 2.5)*	1.25 (1, 2)#
Collagen orientation	TO	1 (1, 1)	2.25 (1, 4)	3.5 (2.5, 4)	2.5 (1, 3.5)
	SA		3 (2.5, 3.5)	2 (1, 3)	1 (1, 1.5)#
Maturity score	TO	6 (6, 6)	16.25 (15, 20.5)	20.25 (17.5, 21)	15.5 (12, 20.5)
	SA		19.5 (17.5, 21.5)	13.25 (11, 17.5)	10 (9.5, 13)#

Abbreviations: SA, suture anchor; TO, transosseous.

*, $p < 0.05$ compared with the TO; #, $p < 0.05$ compared with the 2-week.

As revealed by the biomechanical and histological analyses, both TO and SA technique provided sufficient initial fixation and enabled tendon-to-bone healing, while a significantly better healing of the bone and tendon has been noticed in SA group than TO at 4 weeks. The functional recovery of the two techniques were comparable. Therefore, the hypothesis of this study was partially rejected. Since the SA technique has been widely used in the clinical practice, it is considered of better clinical relevance to investigate new healing enhancements for RC repair on this SA repair model.

4.1 | Healing of the tendon-bone complex

In the present study, the SA group achieved an earlier healing of the tendon-bone complex compared to the TO group, revealed by a significantly higher failure strength and stiffness of the repaired tendon at 4-week post repair. The result of histological analyses also indicated a superior healing of the SA group compared to the TO group at 4-week post repair. The scores of insertion continuity and cell organization of the SA group were significantly higher than TO at 4-week post repair. This finding agreed to a previous study on rabbit that showed the end-point healing of the SA repair was comparable to that of the TO group, but SA group showed a faster healing at 3-week post repair (Barros et al., 2010). It has been reported the SA repair underwent greater motion at the tendon-bone interface than TO, which might result in mechanical stimulations at the interface (Ahmad et al., 2005). (Shi et al., 2012) found that mechanical tensions promoted osteogenic differentiation of rat tendon-derived stem cells. Nakanishi et al. (2019) found increased collagen deposition and tendon-like structures in a tension-loaded condition. Compared to the TO group, whose knot was at the bone shaft distal from the footprint, the suture knot of the SA group was made above the tendon and occupied some space between the acromion and the rotator cuffs, which might compress the tendon onto the bone and lead to better healing. However, these speculations were supported by direct measurements of the present study.

Another probable reason is that the SA surgical procedure only penetrated one side of the cortical bone, while the TO technique perforated both sides. Extra damage of the periosteum would lead to prominent swelling of the tendon and hindered early healing, as found in the gross observation that TO group showed remarkable swelling even at 4-week post repair. Besides, it has been reported that bone marrows promote the tendon-to-bone healing (Kida et al., 2013). In the present study, release of the bone marrow in the SA group might be more than the TO group, as the cancellous bone exposure in SA (0.636 mm^2) was greater than TO (0.318 mm^2). It might explain the SA repair showed better healing of the tendon-bone complex at the early timepoint. At the endpoint, however, both groups showed disorganized fibro-vascular tissue without any continuous fiber between the tendon and bone or distinctive zonal structure of fibrocartilage. Previous studies also found the tendon-bone interface filled with disoriented granulation instead of a typical enthesis after RC repair (Ide & Tokunaga, 2018), so that the biomechanical strength of the repair was inadequate to withstand tensile stresses in functional movements. It seems the positive effect of bone marrow on enthesis healing was insignificant and regeneration of the enthesis remained challenging. The role of bone marrows in RC healing remains a matter of debate.

4.2 | Healing of the bony insertion

On the other hand, healing of the bony tissue of the SA group appeared unsatisfying. The bone parameters decreased significantly after the SA repair and failed to recover to the baseline level even at the endpoint, while those of the TO group did not show significant reduction at any timepoint after repair. The micro-CT indicated the BV of the SA group was significantly less than the TO at 2- and 8-week post repair, indicated an extensive loss of the bone. In the SA group, a large amount of bone mass had been drilled away to prepare the hole, which would lead to a longer healing time than the TO group. The bone loss was considerably less in the TO group. Furthermore, BMD of the SA group was significantly lower than the TO, indicated a poorer bone regeneration at the insertion site. It might be because that the anchor has occupied the space of the hole and hindered the tendon-bone contact. This phenomenon has also been noticed in real patients who suffered from RC retear after SA repair, and insufficient BV regeneration has been regarded as critical factors (Chung et al., 2011; Simon et al., 2003). It is controversial to find the biomechanical property of the bone-to-tendon complex in the SA group was higher while the bone quality was poorer than TO at 4-week post repair. In the biomechanical test, most ruptures took place in the scar tissue instead of the bone, which indicated the weakest link in the tendon-to-bone interface lay at the newly formed soft tissue, but not the formation of the trabecular bone.

4.3 | Functional recovery

No significant difference of walking gait was observed between the groups at all timepoints. The gait has restored to the baseline at 4-week post tear. This finding agreed to the previous study that, after RC tear, the impaired gait would only last for a short time, for example, the swing duration recovered to the baseline within 1 week (Kim et al., 2017; Perry et al., 2009). However, the prompt recovery pattern was much different from those of the patients, most of whom presented progressively decreased shoulder function after injury. After repair, the gait parameters deteriorated for 2 weeks and restored to the baseline at 4-week post repair. This short recovery time might be explained by natural healing capacity of rats. Similar phenomena have been noticed in multiple animal studies with rat models, whose healing progress was proven to be superior to human. Besides, gait analyses reflected shoulder capacity under loading, while human shoulders often underwent a greater range of motion without bearing body weight. Therefore, the newly developed SA technique should be further validated by the functional assessment that is more relevant to human shoulder.

4.4 | Limitations

In this study, the all-suture anchor technique was chosen because the suture is an optimal carrier for biological enhancements in further studies to promote healing after RC tear. However, the healing process after all-suture anchor repair might be different from those of metal or plastic anchors that were commonly used in clinical practice. Therefore, the result of this study should be extrapolated with caution. The material of the suture anchors is absorbable and will be hydrolyzed in 56–70 days (Barbolt, 2002), while the material of all-suture anchors used in humans is non-absorbable. The degradation process might affect the healing process and trigger tissue reactions. Since degradable materials are considered as better solutions for implantations, the interactions between materials and healing need further investigation. Besides, the cross-section of the tendon was not considered in the biomechanical test, because the tissues were in an irregular shape, and it is difficult to identify the tendon from scars. It can be measured by micro-CT or laser devices in previous studies. However, it is hard to keep the tendon under tension during the micro-CT scanning, which may influence the cross-sectional shape of the tendon.

Last, considerable within group standard deviation was presented due to the individual variation of the rats, particularly the functional behavior is very difficult to standardize. It appeared inadequate power of this study, though ratiometric comparison to control limbs within the same animal was used.

5 | CONCLUSIONS

The SA technique is applicable to repair RC tears in rat models. The SA repair achieved faster healing of the RC tendon-bone complex, but not in the bony insertion compared to the TO. The shoulder functions of the SA and TO group are comparable.

AUTHOR CONTRIBUTIONS

Yang LIU, Patrick Shu-Hang Yung contributed to the conception of the study; Yang LIU, Shi-Yi YAO performed the experiment; Yang LIU, Sai-Chuen FU contributed significantly to analysis and manuscript preparation; Yang LIU, Sai-Chuen FU, Xiao-Dan CHEN performed the data analyses and wrote the manuscript; Yang LIU, Sai-Chuen FU helped perform the analysis with constructive discussions. This research did not receive any specific grant from funding agencies in the public, commercial, or not-for-profit sectors, and no material support of any kind was received.

ACKNOWLEDGMENTS

We would like to thank for Ming-Yan LI, Kwan-Pui TANG, and Hong-Tao XU for assisting conduct the animal surgeries. We would like to thank Yau-Chuk CHEUK for technical support in histological analysis. The first author Yang Liu would like to thank, in particular, the invaluable support received from Dr. Yu Pan over the whole period of this work.

CONFLICTS OF INTEREST

The authors have no potential sources of conflicts of interest relevant to this article.

DATA AVAILABILITY STATEMENT

Research data are not shared.

ORCID

Yang Liu https://orcid.org/0000-0003-3831-7153
Sai-Chuen Fu https://orcid.org/0000-0001-5865-6801
Shi-Yi Yao https://orcid.org/0000-0003-4134-0370
Xiao-Dan Chen https://orcid.org/0000-0003-0409-6516
Patrick Shu-Hang Yung https://orcid.org/0000-0002-7214-5503

REFERENCES

Ahmad, C. S., Stewart, A. M., Izquierdo, R., & Bigliani, L. U. (2005). Tendon-bone interface motion in transosseous suture and suture anchor rotator cuff repair techniques. *The American Journal of Sports Medicine*, *33*(11), 1667–1671. https://doi.org/10.1177/0363546505278252

Barber, F. A., & Herbert, M. A. (2017). All-suture anchors: Biomechanical analysis of pullout strength, displacement, and failure mode. *Arthroscopy*, *33*(6), 1113–1121. https://doi.org/10.1016/j.arthro.2016.09.031

Barbolt, T. A. (2002). Chemistry and safety of triclosan, and its use as an antimicrobial coating on Coated VICRYL* Plus Antibacterial Suture (coated polyglactin 910 suture with triclosan). *Surgical Infections*, *3*(s1), S45–S53. https://doi.org/10.1089/sur.2002.3.s1-45

Barros, R. M., Matos, M. A., Ferreira Neto, A. A., Benegas, E., Guarniero, R., Pereira, C. A., & Bolliger Neto, R. (2010). Biomechanical evaluation on tendon reinsertion by comparing trans-osseous suture and suture anchor at different stages of healing: Experimental study on rabbits. *Journal of Shoulder and Elbow Surgery*, *19*(6), 878–883. https://doi.org/10.1016/j.jse.2010.03.008

Bedeir, Y. H., Jimenez, A. E., & Grawe, B. M. (2018). Recurrent tears of the rotator cuff: Effect of repair technique and management options. *Orthopedic Reviews*, *10*(2), 7593. https://doi.org/10.4081/or.2018.7593

Bedi, A., Kovacevic, D., Hettrich, C., Gulotta, L. V., Ehteshami, J. R., Warren, R. F., & Rodeo, S. A. (2010). The effect of matrix metalloproteinase inhibition on tendon-to-bone healing in a rotator cuff repair model. *Journal of Shoulder and Elbow Surgery*, *19*(3), 384–391. https://doi.org/10.1016/j.jse.2009.07.010

Burkhart, S. S., Diaz Pagan, J. L., Wirth, M. A., & Athanasiou, K. A. (1997). Cyclic loading of anchor-based rotator cuff repairs: Confirmation of the tension overload phenomenon and comparison of suture anchor fixation with transosseous fixation. *Arthroscopy*, *13*(6), 720–724. https://doi.org/10.1016/s0749-8063(97)90006-2

Chung, S. W., Oh, J. H., Gong, H. S., Kim, J. Y., & Kim, S. H. (2011). Factors affecting rotator cuff healing after arthroscopic repair: Osteoporosis as one of the independent risk factors. *The American Journal of Sports Medicine*, *39*(10), 2099–2107. https://doi.org/10.1177/0363546511415659

Cj, L., & K, Y. (2002). Natural history and nonsurgical treatment of rotator cuff disorders. In N. TR (Ed.), *Orthopaedic knowledge update: Shoulder and elbow 2* (Vol. 2, pp. 155–162). Amer Academy of Orthopaedic.

Denard, P. J., & Burkhart, S. S. (2013). The evolution of suture anchors in arthroscopic rotator cuff repair. *Arthroscopy*, *29*(9), 1589–1595. https://doi.org/10.1016/j.arthro.2013.05.011

Easley, J., Puttlitz, C., Hackett, E., Broomfield, C., Nakamura, L., Hawes, M., Getz, C., Frankle, M., St Pierre, P., Tashjian, R., Cummings, P. D., Abboud, J., Harper, D., & McGilvray, K. (2020). A prospective study comparing tendon-to-bone interface healing using an interposition bioresorbable scaffold with a vented anchor for primary rotator cuff repair in sheep. *Journal of Shoulder and Elbow Surgery*, *29*(1), 157–166. https://doi.org/10.1016/j.jse.2019.05.024

Ficklscherer, A., Loitsch, T., Serr, M., Gulecyuz, M. F., Niethammer, T. R., Muller, H. H., Milz, S., Pietschmann, M. F., & Muller, P. E. (2014). Does footprint preparation influence tendon-to-bone healing after rotator cuff repair in an animal model? *Arthroscopy*, *30*(2), 188–194. https://doi.org/10.1016/j.arthro.2013.11.016

Fu, S. C., Cheuk, Y. C., Hung, L. K., & Chan, K. M. (2012). Limb idleness index (LII): A novel measurement of pain in a rat model of osteoarthritis. *Osteoarthritis and Cartilage*, *20*(11), 1409–1416. https://doi.org/10.1016/j.joca.2012.08.006

Gerber, C., Schneeberger, A. G., Beck, M., & Schlegel, U. (1994). Mechanical strength of repairs of the rotator cuff. *Journal of Bone and Joint Surgery British Volume*, *76*(3), 371–380. https://doi.org/10.1302/0301-620X.76B3.8175836

Harrison, J. A., Wallace, D., Van Sickle, D., Martin, T., Sonnabend, D. H., & Walsh, W. R. (2000). A novel suture anchor of high-density collagen compared with a metallic anchor. Results of a 12-week study in sheep. *The American Journal of Sports Medicine*, *28*(6), 883–887. https://doi.org/10.1177/03635465000280061801

Ide, J., & Tokunaga, T. (2018). Rotator cuff tendon-to-bone healing at 12 months after patch grafting of acellular dermal matrix in an animal model. *Journal of Orthopaedic Science*, *23*(2), 207–212. https://doi.org/10.1016/j.jos.2017.11.018

Kang, Y. G., Kim, J. H., Shin, J. W., Baik, J. M., & Choo, H. J. (2013). Induction of bone ingrowth with a micropore bioabsorbable suture anchor in rotator cuff tear: An experimental study in a rabbit model. *Journal of Shoulder and Elbow Surgery*, *22*(11), 1558–1566. https://doi.org/10.1016/j.jse.2013.01.034

Kida, Y., Morihara, T., Matsuda, K., Kajikawa, Y., Tachiiri, H., Iwata, Y., Sawamura, K., Yoshida, A., Oshima, Y., Ikeda, T., Fujiwara, H., Kawata, M., & Kubo, T. (2013). Bone marrow-derived cells from the footprint infiltrate into the repaired rotator cuff. *Journal of Shoulder and Elbow Surgery*, *22*(2), 197–205. https://doi.org/10.1016/j.jse.2012.02.007

Kim, S. J., Lee, S. M., Kim, J. E., Kim, S. H., & Jung, Y. (2017). Effect of platelet-rich plasma with self-assembled peptide on the rotator cuff tear model in rat. *Journal of tissue engineering and regenerative medicine*, *11*(1), 77–85. https://doi.org/10.1002/term.1984

Kovacevic, D., Fox, A. J., Bedi, A., Ying, L., Deng, X. H., Warren, R. F., & Rodeo, S. A. (2011). Calcium-phosphate matrix with or without TGF-beta3 improves tendon-bone healing after rotator cuff repair. *The American Journal of Sports Medicine*, *39*(4), 811–819. https://doi.org/10.1177/0363546511399378

Levy, D. M., Saifi, C., Perri, J. L., Zhang, R., Gardner, T. R., & Ahmad, C. S. (2013). Rotator cuff repair augmentation with local autogenous bone marrow via humeral cannulation in a rat model. *Journal of Shoulder and Elbow Surgery*, *22*(9), 1256–1264. https://doi.org/10.1016/j.jse.2012.11.014

Lipner, J., Shen, H., Cavinatto, L., Liu, W., Havlioglu, N., Xia, Y., Galatz, L. M., & Thomopoulos, S. (2015). In vivo evaluation of adipose-derived stromal cells delivered with a nanofiber scaffold for tendon-to-bone repair. *Tissue Engineering Part A*, *21*(21–22), 2766–2774. https://doi.org/10.1089/ten.TEA.2015.0101

McElvany, M. D., McGoldrick, E., Gee, A. O., Neradilek, M. B., & Matsen, F. A., 3rd (2015). Rotator cuff repair: Published evidence on factors associated with repair integrity and clinical outcome. *The American Journal of Sports Medicine*, *43*(2), 491–500. https://doi.org/10.1177/0363546514529644

Mergenthaler, P., & Meisel, A. (2015). Animal models. In *Principles of translational science in medicine* (pp. 83–90).

Min, H. K., Kwon, O. S., Oh, S. H., & Lee, J. H. (2016). Platelet-derived growth factor-BB-immobilized asymmetrically porous membrane for enhanced rotator cuff tendon healing. *Tissue engineering and regenerative medicine*, *13*(5), 568–578. https://doi.org/10.1007/s13770-016-9120-3

Moosmayer, S., Lund, G., Seljom, U. S., Haldorsen, B., Svege, I. C., Hennig, T., Pripp, A. H., & Smith, H. J. (2019). At a 10-year follow-up, tendon

repair is superior to physiotherapy in the treatment of small and medium-sized rotator cuff tears. *JBJS*, *101*(12), 1050–1060. https://doi.org/10.2106/JBJS.18.01373

Nakanishi, Y., Okada, T., Takeuchi, N., Kozono, N., Senju, T., Nakayama, K., & Nakashima, Y. (2019). Histological evaluation of tendon formation using a scaffold-free three-dimensional-bioprinted construct of human dermal fibroblasts under in vitro static tensile culture. *Regenerative therapy*, *11*, 47–55. https://doi.org/10.1016/j.reth.2019.02.002

Park, M. C., Cadet, E. R., Levine, W. N., Bigliani, L. U., & Ahmad, C. S. (2005). Tendon-to-bone pressure distributions at a repaired rotator cuff footprint using transosseous suture and suture anchor fixation techniques. *The American Journal of Sports Medicine*, *33*(8), 1154–1159. https://doi.org/10.1177/0363546504273053

Perry, S. M., Getz, C. L., & Soslowsky, L. J. (2009). Alterations in function after rotator cuff tears in an animal model. *Journal of Shoulder and Elbow Surgery*, *18*(2), 296–304. https://doi.org/10.1016/j.jse.2008.10.008

Shi, Y., Fu, Y., Tong, W., Geng, Y., Lui, P. P., Tang, T., Zhang, X., & Dai, K. (2012). Uniaxial mechanical tension promoted osteogenic differentiation of rat tendon-derived stem cells (rTDSCs) via the Wnt5a-RhoA pathway. *Journal of Cellular Biochemistry*, *113*(10), 3133–3142. https://doi.org/10.1002/jcb.24190

Simon, D., Pitsillidies, A., Emery, R., & Wallace, A. (2003). Local osteoporosis after rotator cuff tear. *Orthopaedic Proceedings*, *85-B*(SUPP I), 10. https://doi.org/10.1302/0301-620X.85BSUPP_I.0850010a

Soslowsky, L. J., Carpenter, J. E., DeBano, C. M., Banerji, I., & Moalli, M. R. (1996). Development and use of an animal model for investigations on rotator cuff disease. *Journal of Shoulder and Elbow Surgery*, *5*(5), 383–392. https://doi.org/10.1016/s1058-2746(96)80070-x

Vastamaki, M., Lohman, M., & Borgmastars, N. (2013). Rotator cuff integrity correlates with clinical and functional results at a minimum 16 years after open repair. *Clinical Orthopaedics and Related Research*, *471*(2), 554–561. https://doi.org/10.1007/s11999-012-2494-1

Vidt, M. E., Santago, A. C., II, Marsh, A. P., Hegedus, E. J., Tuohy, C. J., Poehling, G. G., Freehill, M. T., Miller, M. E., & Saul, K. R. (2016). The effects of a rotator cuff tear on activities of daily living in older adults: A kinematic analysis. *Journal of Biomechanics*, *49*(4), 611–617. https://doi.org/10.1016/j.jbiomech.2016.01.029

Visscher, L. E., Jeffery, C., Gilmour, T., Anderson, L., & Couzens, G. (2019). The history of suture anchors in orthopaedic surgery. *Clinical biomechanics*, *61*, 70–78. https://doi.org/10.1016/j.clinbiomech.2018.11.008

Yamamoto, A., Takagishi, K., Osawa, T., Yanagawa, T., Nakajima, D., Shitara, H., & Kobayashi, T. (2010). Prevalence and risk factors of a rotator cuff tear in the general population. *Journal of Shoulder and Elbow Surgery*, *19*(1), 116–120. https://doi.org/10.1016/j.jse.2009.04.006

Yonemitsu, R., Tokunaga, T., Shukunami, C., Ideo, K., Arimura, H., Karasugi, T., Nakamura, E., Ide, J., Hiraki, Y., & Mizuta, H. (2019). Fibroblast growth factor 2 enhances tendon-to-bone healing in a rat rotator cuff repair of chronic tears. *The American Journal of Sports Medicine*, *47*(7), 1701–1712. https://doi.org/10.1177/0363546519836959

How to cite this article: Liu, Y., Fu, S.-C., Yao, S.-Y., Chen, X.-D., & Yung, P. S.-H. (2022). Application of suture anchors for a clinically relevant rat model of rotator cuff tear. *Journal of Tissue Engineering and Regenerative Medicine*, *16*(8), 757–770. https://doi.org/10.1002/term.3326